Title	Shape Optimization of Ceramics/Metal Joint Based on Reliability(Mechanics, Strength & Structural Design)
Author(s)	Murakawa, Hidekazu; Ueda, Yukio
Citation	Transactions of JWRI. 1990, 19(2), p. 231-239
Version Type	VoR
URL	https://doi.org/10.18910/5260
rights	
Note	

Osaka University Knowledge Archive : OUKA

https://ir.library.osaka-u.ac.jp/

Osaka University

Shape Optimization of Ceramics/Metal Joint Based on Reliability

Hidekazu MURAKAWA* and Yukio UEDA**

Abstract

Due to their brittleness and poor machinability, ceramics are used in the form of composite structure with metals. However, stress concentration occurs in the region near the edge of interface between the ceramics and the metal. Such high stress may cause cracking of ceramics under thermal loads and reduce the reliability under external loads. In general, the stress concentration greatly depends on the geometry or the shape of the joint.

The authors investigated the possibility of reducing the failure probability through controlling the shape of the joint. For this purpose, the problem is treated as an optimization problem and a shape optimization procedure in which the failure probability is minimized is proposed. Further, it is applied to simple example problems, which can be considered as linear thermal-elastic problems, to show that the proposed optimization technique can be an useful tool to desigh shapes of joints between dissimilar materials.

KEY WORDS: (Shape Optimization) (Optimum Design) (Reliability) (Ceramics/Metal Joint) (Finite Element Method)

1. Introduction

New-Ceramics have a great potential in various engineering applications. However, most ceramics are brittle and poor in machinability. These drawbacks are overcome by introducing composite structure consisting of ceramics and metal. In most cases, ceramics and metal are joined at elevated temperature by methods such as brazing or diffusion bonding. Due to the large difference in thermal expansion coefficients of the two materials, significant magnitude of residual stress is produced during the cooling process after joining[1]. Such residual stress created at the bonding region may cause cracking or reduce the bonding strength. Thus, it is desirable to minimize the size of the residual stress and various techniques are developed for this purpose. One such technique is to introduce an interlayer[2]. Another possible technique is to reduce stress by controlling the shape of the bonding zone[3].

The authors treated the problem of reducing the residual stress through shape control as an optimum design problem and developed a numerical method to automatically determine the optimum shape for the given conditions[4]. In this method, shape is optimized based on a simple assumption that the ceramics break when the maximum stress reaches the critical value. However, the strength of the ceramics shows statistical variations. For this reason, statistical approaches[5] are widely employed in strength evaluation of ceramics parts.

Considering such statistical nature of ceramics, a new optimization technique based on the probabilistic evaluation of reliability is proposed in this paper. The failure probability is employed as an objective function and the shape which minimizes it is sought as an optimum shape.

2. Shape Optimization Method

2.1 Representation of shape and its modifivation

The two dimensional shape optimization problem, shown in **Fig. 1**, is considered. In this report, both ceramic and metal parts are assumed to be cylindrical and joined coaxially, so that the problem can be treated as axisymmetric thermal-elastic problems. The shapes of the ceramic and the metal parts are represented by the lines in $r-z$ plane which correspond to surfaces and interface of the materials.

The domain for the stress analysis is subdivided into a finite number of elements (3 node triangular Finite Elements are used in this report) and nodes are defined at the corners of the elements. Since the nodes are also defined on the surface and the interface, the shape of the joint can be represented by their coordinates. Further, the modification of the shape can be achieved by moving these nodes. If the part of the boundary to
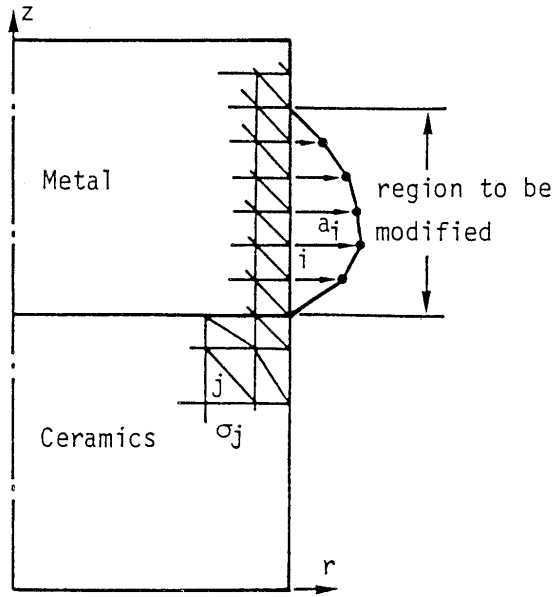
Fig. 1 Description of shape and its modification.

be modified and the directions in which the nodes can move are given a priori, the modified shape can be uniquely defined by the distance of move a_i of the i—th node. In other words, the shape can be defined by a_i as design parameters.

2.2 Failure probability and constraint condition

(1) failure probability

As one of the methods to evaluate the strength of brittle materials such as creamics, methods based on the weakest link hypothesis and the statistics have been proposed[5]. For example, if three modes of failure, namely, those initiated from internal cracks, surface cracks and edge cracks, are considered, the failure probability P_f can be estimated by the following equation.

$$P_f = 1 - \exp\left(-B_1 - B_2 - B_3\right) \qquad (1)$$

In the above equations, B_1, B_2 and B_3 are hazard functions for respective failure mode and defined by,

$$B_1 = \int_V \left(\frac{\sigma - \sigma_{u1}}{\sigma_{01}}\right)^{m1} Y(\sigma, \sigma_{u1}) dv$$

$$B_2 = \int_A \left(\frac{\sigma - \sigma_{u2}}{\sigma_{02}}\right)^{m2} Y(\sigma, \sigma_{u2}) dA \qquad (2)$$

$$B_3 = \int_L \left(\frac{\sigma - \sigma_{u3}}{\sigma_{03}}\right)^{m3} Y(\sigma, \sigma_{u3}) dL$$

where, σ represents the maximum principal stress at arbitrary points, and m_i, σ_{0i}, σ_{ui} ($i=1, 2, 3$) are parameters for the three parameter Weibull distribution. The integrals $\int dv, \int dA, \int dL$ represent those over the

volume, the surface and the edge length of the ceramics part, respectively.

The Function $Y(\sigma, \sigma_{ui})$ is the heaviside step function. For simplicity, only the failure mode due to the internal cracks is consider in the following discussion. In other words, only B_1 is considered in Eq. (1). Further, it is assumed that $\sigma_{ui}=0$. Using the maximum principal stress σ_j computed for each element, the failure probability P_f can be estimated as,

$$F = 1 - \exp\left\{-\int (\sigma/\sigma_{01})^m Y(\sigma_j, 0) dv\right\}$$

$$= 1 - \exp\left\{-\sum_j v_j (\sigma_j/\sigma_{01})^m Y(\sigma_j, 0)\right\} \qquad (3)$$

where, $v_j = 2\pi r A_j$ and A_j is the area of the j-th element.

(2) constraining condition

In case of practical engineering problems, there are certain restrictions so that the product can be machined or produced and fulfill the required function. The shape of the product is also subjected to various constraints. As one of the geometrical constraints, the arc length is assumed to be constant and the optimum shape is sought under this condition. In other words, when the original arc length is L_0, the arc length of the optimum shape is kept αL_0, where α is a given constant and referred to as arc length factor.

2.3 Optimization problem and objective function

(1) optimization problem with subsidiary condition

The optimization problem can be stated that, to determine the shape for which the objective function W, which is the failure probability P_f in this case, is minimized under the given constraint condition, i.e.

$$W = P_f \Rightarrow \min \qquad (4)$$

under the following condition forced on the arc length of the boundary to be optimized.

$$L = \alpha L_0 \qquad (5)$$

However, this condition is nonlinear and it is difficult to satisfy a priori. To overcome this difficulty, the optimization problem is modified to that without subsidiary condition.

(2) optimization problem without subsidiary condition

By introducing the Lagrange multiplier λ, the subsidiary condition can be embedded in the objective function and the new objective function W^* in the following form is derived.

$$W^*(a_i, \lambda) = 1 - \exp\left[-\sum v_j \{\sigma_j(a_i)/\sigma_{01}\}^m\right]$$

$$-\lambda \{L(a_i) - \alpha L_0\} \qquad (6)$$

Using the above objective function, the subsidiary condition can be removed from the optimization problem and the optimum solution is obtained by simply minimizing the objective function $W^*(a_i, \lambda)$. For convenience, Eq. (6) is rewritten in the following form.

$$W^*(a_i, \lambda) = 1 - f(\sum g_j(\sigma_j(a_i)))$$
$$- \lambda\{L(a_i) - \alpha L_0\} \qquad (7)$$

where,

$f = \exp(\sum g_j)$

$g_j = v_j\{\sigma_j(a_i)/\sigma_{01}\}^m$

$\sum$: summation over the elements in the ceramic part where the maximum principal stress is positive.

a_i : moving distance of the i-th node which locates on the boundary to be optimized.

2.4 Iterative procedure

Since the objective function W^* given by Eq. (6) is a highly nonlinear function in terms of a_i and λ, its stationarity conditions, i.e.

$$\partial W^*/\partial a_i = 0, \quad \partial W^* \partial/\lambda = 0 \qquad (8)$$

also become nonlinear, it is impossible to solve these equations in a single step. Thus, the optimum solution is sought through an iterative procedure. If the approximate values obtained after the (n)th iteration are denoted by a_i^n and λ^n, these are corrected by Δa_i and $\Delta\lambda$ in the $(n+1)$th iteration to get new approximations a_i^{n+1} and λ^{n+1}, such that,

$$a_i^{n+1} = a_i^n + \Delta a_i, \quad \lambda^{n+1} = \lambda^n + \Delta\lambda \qquad (9)$$

Considering the objective function W^* as a function of Δa_i and $\Delta\lambda$, it can be expanded in Taylor series. If the terms higher than the second order terms in Δa_i and $\Delta\lambda$ are neglected, the objective function W^* is reduced to,

$$W^*(\Delta a_i, \Delta\lambda) = W_0^*(a_j^n, \lambda^n) + W_1^*(\Delta a_i, \Delta\lambda)$$
$$+ W_2^*(\Delta a_i, \Delta\lambda) \qquad (10)$$

where, W_0^*, W_1^* and W_2^* represent the constant, the first order and the second order terms in Δa_i and $\Delta\lambda$, respectively, i.e.

$$W_0^* = W^*(a_i, \lambda)$$

$$W_1^* = -\frac{\partial f}{\partial a_p}\Delta a_p - \lambda\frac{\partial L}{\partial a_p}\Delta a_p - \Delta\lambda\{L - \alpha L_0\}$$

$$= -\sum\frac{\partial f}{\partial g}\frac{dg_i}{d\sigma_i}\frac{\partial\sigma_i}{\partial a_p}\Delta a_p - \lambda\frac{\partial L}{\partial a_p}\Delta a_p$$

$$- \Delta\lambda\{L - \alpha L_0\}$$

$$W_2^* = -\frac{1}{2}\frac{\partial^2 f}{\partial a_p\partial a_q}\Delta a_p\Delta a_q - \frac{\lambda}{2}\frac{\partial^2 L}{\partial a_p\partial a_q}\Delta a_p\Delta a_q$$
$$- \Delta\lambda\frac{\partial L}{\partial a_p}\Delta a_p$$

$$= -\frac{1}{2}\Big[\sum\Big(\frac{\partial^2 f}{\partial g_i\partial g_j}\Big)\Big(\frac{dg_i dg_j}{d\sigma_i d\sigma_j}\Big)\Big(\frac{\partial\sigma_i}{\partial a_p}\Big)\Big(\frac{\partial\sigma_j}{\partial a_q}\Big)$$
$$+ \sum\frac{\partial f}{\partial g}\Big(\frac{d^2 g_i}{d\sigma_i^2}\Big)\Big(\frac{\partial\sigma_i}{\partial a_p}\Big)\Big(\frac{\partial\sigma_i}{\partial a_q}\Big)$$
$$+ \sum\frac{\partial f}{\partial g_i}\Big(\frac{dg_i}{d\sigma_i}\Big)\Big(\frac{\partial^2\sigma_i}{\partial a_p\partial a_q}\Big)\Big]\Delta a_p\Delta a_q$$
$$- \frac{\lambda}{2}\frac{\partial^2 L}{\partial a_p a\partial_q}\Delta a_p\Delta a_q - \Delta\lambda\frac{\partial L}{\partial a_p}\Delta a_p$$

The derivatives of f and g are given by,

$$\frac{\partial f}{\partial g_i} = f$$

$$\frac{\partial^2 f}{\partial g_i} = f$$

$$\frac{\partial^2 f}{\partial g_i\partial g_j} = f$$

$$\frac{dg_i}{d\sigma_i} = -m\Big(\frac{V_i}{\sigma_{01}}\Big)\Big(\frac{\sigma_i}{\sigma_{01}}\Big)^{m-1}$$

$$\frac{d^2 g_i}{d\sigma_i^2} = -m(m-1)\Big(\frac{V_i}{\sigma_{01}^2}\Big)\Big(\frac{\sigma_1}{\sigma_{01}}\Big)^{m-2}$$

The above objective function, which is expanded in the Taylor series up to the second order terms, cam be rewritten in the following matrix form.

$$W^*(\Delta a_i, \Delta\lambda) = W_0^*(a_i^n, \lambda^n) - \begin{Bmatrix}\Delta a_i \\ \Delta\lambda\end{Bmatrix}^T \begin{Bmatrix}F_a \\ F_b\end{Bmatrix}$$
$$+ \frac{1}{2}\begin{Bmatrix}\Delta a_i \\ \Delta\lambda\end{Bmatrix}^T \begin{vmatrix}K_{aa} & K_{ab} \\ K_{ba} & K_{bb}\end{vmatrix}\begin{Bmatrix}\Delta a_k \\ \Delta\lambda\end{Bmatrix} \qquad (11)$$

Using the stationarity condition, such that,

$$\partial W^*/\partial\Delta a_i = 0, \quad \partial W^*/\partial\Delta\lambda = 0 \qquad (12)$$

a set of linear algebraic equations in terms of Δa_i, $\Delta\lambda$ are derived.

$$\begin{vmatrix}K_{aa} & K_{ab} \\ K_{ba} & K_{bb}\end{vmatrix}\begin{Bmatrix}\Delta a_i \\ \Delta\lambda\end{Bmatrix} = \begin{Bmatrix}F_a \\ F_b\end{Bmatrix} \qquad (13)$$

By solving the above equation, Δa_i, $\Delta\lambda$ are determined and the new approximate solution a_i^{n+1}, λ^{n+1} can be obtained from Eq. (9). Further, the optimum solution for the given arc length αL_0 can be obtained by repeating the same procedure until the convergence is reached.

2.5 Optimality of the solution

The formulation and the optimization procedure is

shown in the preceding section. In this section, the optimality and the meaning of the solution is examined.

In general, optimum solution is the solution whcih minimizes the objective function among all the possible alternatives which satisfy the given constraint conditions. Thus, for the optimality in the strict sense, the objective function must be defined in such a way that any subjective or ambiguous element is excluded. Also, the solution must be searched among all the possible alternatives.

In this section, objectivity of the objective functions which are used in the last[4] and the present reports are examined. The objective function proposed in the previous paper is shown in the following.

$$W^*(a_i, \lambda) = \sum_j A_j \{w_j(a_i)\}^2 - \lambda \{L(a_i) - \alpha L_0\} \quad (14)$$

where,

$$w_j =: \sigma_j - \sigma_0 \quad \text{if} \quad \sigma_j > \sigma_0$$
$$w_j = 0 \quad \text{if} \quad \sigma_j \leqq \sigma_0$$

The above function W^* represents the weighted square sum of $w_j = \sigma_j - \sigma_0$, which is the stress exceeding the given objective allowable stress σ_0. Considering that this type of objective function involves σ_0 and A_i as rather arbitrary given constants and the physical meaning of the square sum of w_j is ambiguous, it can not be fully acceptable as a proper objective function.

In contrast to this, the objective function proposed in this report possesses clear physical meaning and it represents the failure probability. Further, the Weibull parameters σ_{01} and m_1 involved in the failure probability can be determined as material constants through experiment. Therefore, the function given by Eq. (6) can be considered as an objective measure of optimality and the optimum solution obtained based on it has a generally acceptable meaning.

3. Example of Shape Optimization

3.1 Example model

Numerical results of optimization are presented for simple example problems. The model for the example problems is shown in **Fig. 2**. It consists of ceramics (Al_2O_3) and metal (Cu) parts with the same size. Their height and the diameter are 10 mm and 20 mm, respectively. It is assumed that the variations of material constants with temperature can be neglected and the values at room temperature are used. **Table 1** shows the Young's moduli, Poison's ratios and thermal expansion coefficients for the two materials. The parameters of Weibull distribution which determines the
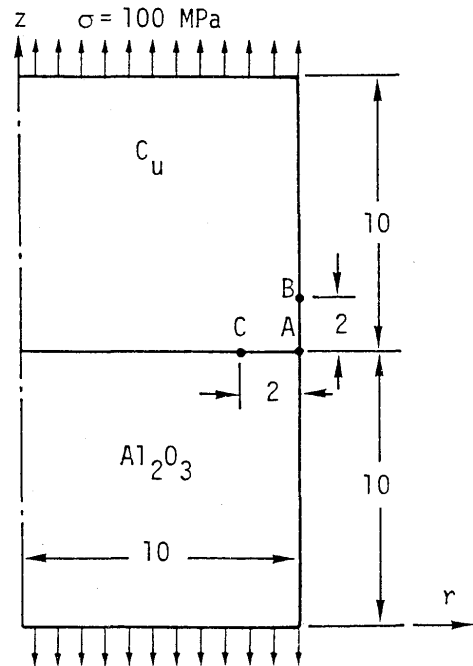

Fig. 2 Example model and region to be modified.

Table 1 Mechanical properties of materials.

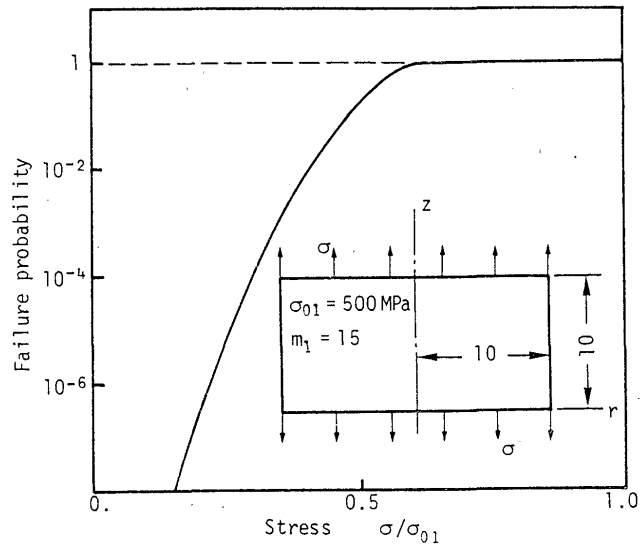|	Al_2O_3	Cu
Young's modulus (GPa)	370	130
Poisson's ratio	0.25	0.3
Thermal expansion coef. (1/K)	7.9×10^{-6}	17.7×10^{-6}

Fig. 3 Failure probability of ceramic cylinder under uniform tension.

failure probability of the ceramic part, are assumed to be,

$$\sigma_{01} = 500 \ MPa, \quad m_1 = 15$$

The above assumed values are not measured ones.

They are arbitrarily assumed fictitious values. The failure probability of a cylindrical specimen made of such material under uniform tensile load is plotted against the applied stress σ in **Fig. 3**. The size of the specimen is same as the above example. Its radius and height are same and assumed to be 10 mm.

3.2 Condition of optimization

The shapes are optimized under the conditions which are given as the combination of the following loading conditions and the constraint conditions on the part of the boundary to be modified.

loading condition

(1) uniform tensile stress of 100 MPa is acting as an external load

(2) thermal stress due to temperature drop by 100°C

(3) both (1) and (2) are acting simultaneously

boundary to be modified

(1) side surface of the metal part 2 mm from the interface (A-B in Fig. 2)

(2) part of the interface 2 mm from the edge (A-C in Fig. 2)

arc length: L

$$L = 1.005 \, L_0 \sim 1.10 \, L_0$$

3.3 Procedure of optimization

The procedure of optimization is shown using the problem under the uniform tensile force. The applied stress is 100 MPa and the side surface of the metal is optimized in this case. The distribution of the largest principal stress for the original shape is shown in **Fig.4**. the maximum stress in the ceramics part occurs at the point P on the edge of the interface and its value σ_{max} is 165 MPa. The failure probability of the joint P_f is 3.07×10^{-7}. As it was mentioned earlier, the optimum shape is obtained through iteration based on linealized approximation. Hence, it is necessary to give a set of proper initial values. The following values are used as initial values.

$$a_i = 0, \quad \lambda = \pm 10^4$$

As the first case, the shape is optimized for $\alpha = 1.005$. Then, this optimum solution is used as the initial value for the case in which $\alpha = 1.01$. The optimum shapes for larger values of the arc length factor ($\alpha = 1.02$, 1.05, 1.10) are computed successively in the same manner.

The optimized shapes and the failure probability after optimization are shown for different values of arc length factor in **Fig. 5**. In case of this example, concave shapes are obtained as optimum shape when positive value is chosen as the initial value of λ and
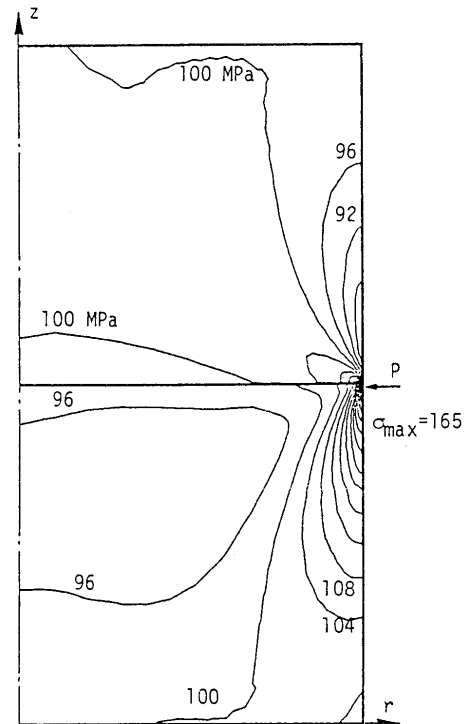

Fig. 4 Distribution of the largest principal stress in the original model under uniform external load.
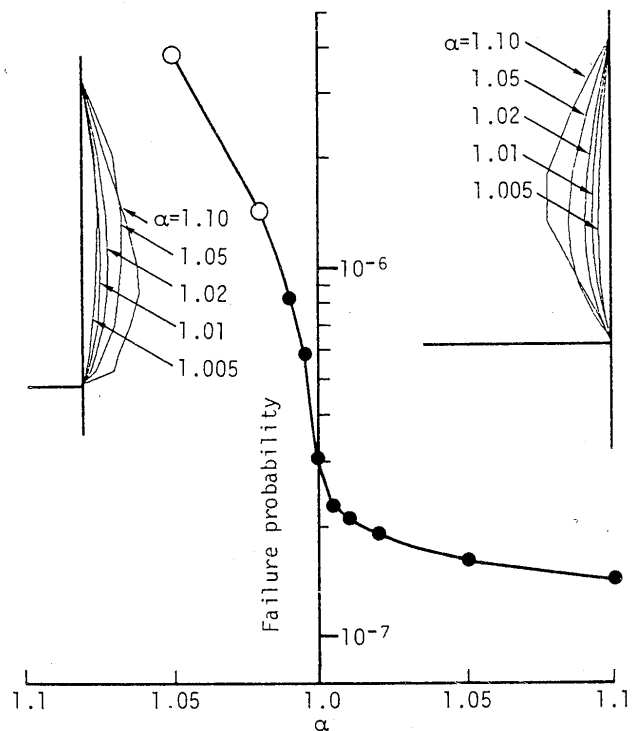

Fig. 5 Optimum shapes and the failure probability under uniform external load.

convex shapes are obtained viceversa. When the optimum shape is concave, converged solution is obtained reregardless of the value of the arc length factor α. On the hand, fully converged solution is not obtained if the shape is convex and α is larger than 1.02. Such

cases for which the convergence is not reached are shown by open circles and those for which converged
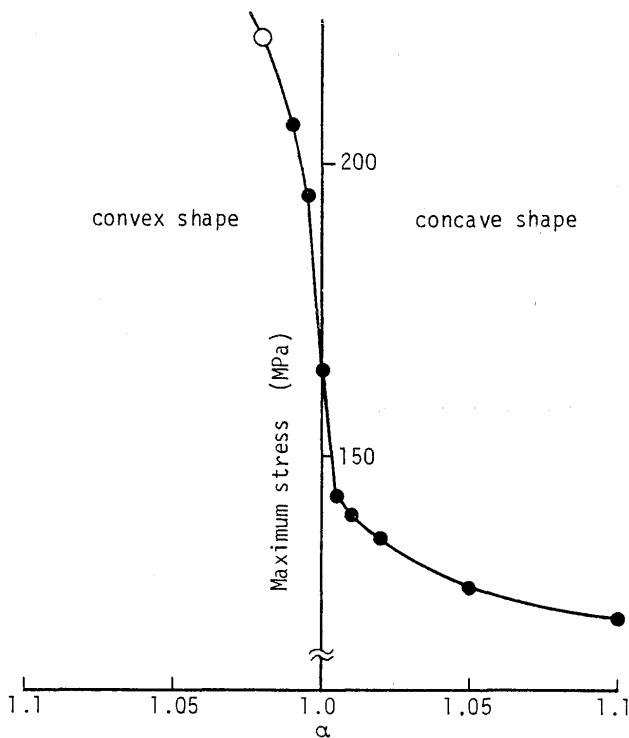

Fig. 6   Variation of the maximum stress in ceramics under external load with arc length factor.
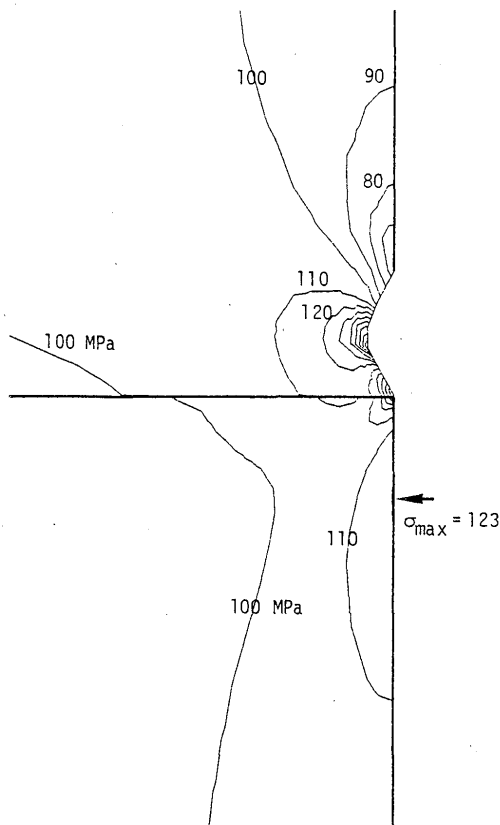

Fig. 7   Distribution of the largest principal stress in the optimum shape under uniform external load ($\alpha=1.10$).

solution is obtained are shown by solid circles in Fig.5. It can be seen from Fig. 5 that the failure probability decreases with the increase of arc length factor when the shape is concave. The failure probability becomes 1.46×10^{-7} which is about the half of the failure probability before optimization. On the contrary, when the shape is convex, it rapidly increases with the arc length factor.

For reference, the relation between the maximum tensile stress in ceramic part σ_{max} and the arc length factor α is shown in **Fig. 6**. The maximum stress is roughly reduced by 25% when shape is concave and $\alpha=1.10$. The distribution of the largest principal stress for the same case is shown in **Fig. 7**. Comparing Figs. 4 and 7, it can be seen that the location of the point where the maximum stress exists moves away from the interface and the stress at the edge of the interface is relaxed.

3.4 Loading condition and optimum shape

In the preceding section, optimum shapes are computed for the case in which uniform external load is applied and it is shown that the stress is reduced when the shape is concave and the ratio of reduction increases with the arc length factor α. In other words, it decreases with the depth of the notch. However, it is expected that the optimum shape changes with the loading condition. To investigate the effect of the loading condition, shapes are optimized under different loading conditions. Two loading conditions, namely, the cases in which thermal load due to the temperature drop by 100°C is acting and both thermal and external loads are acting simultaneously, are considered. For the case under the thermal load, the distribution of the largest principal stress before the optimization is shown in **Fig. 8**. The maximum tensile stress σ_{max} in the ceramics part occurs at point P and its value is 324 MPa. The failure probability P_f in this case is 3.31×10^{-4}. The results of the optimization are shown in **Fig. 9** and **10**. Unlike the case under external load, the failure probability reduces when the shape is convex. When the shape is concave, fully converged solution is obtained only for $\alpha=1.08$ and the failure probability is decreased compared to the original shape. Such characteristics are also observed in the optimization based on the objective function given by Eq. (14) which is discussed in the previous paper[4].

When both the thermal and external loads are acting, the distribution of the maximum principal stress for the original shape is computed and shown in **Fig. 11**. The maximum stress in the ceramic part and the failure probability are $\sigma_{max}=479$ MPa and $P_f=0.21$ respec-
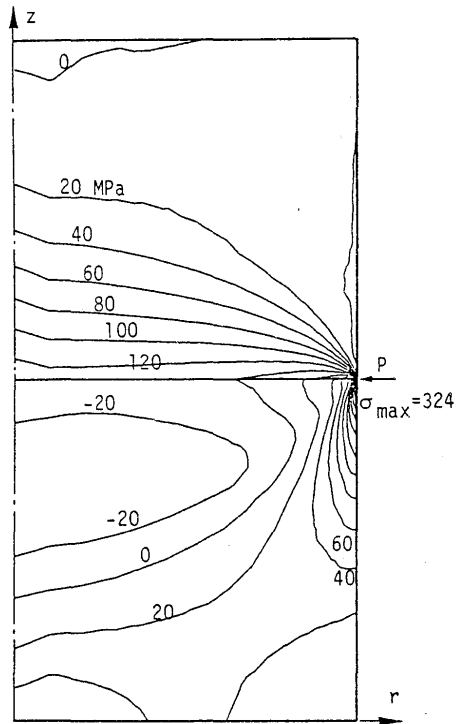
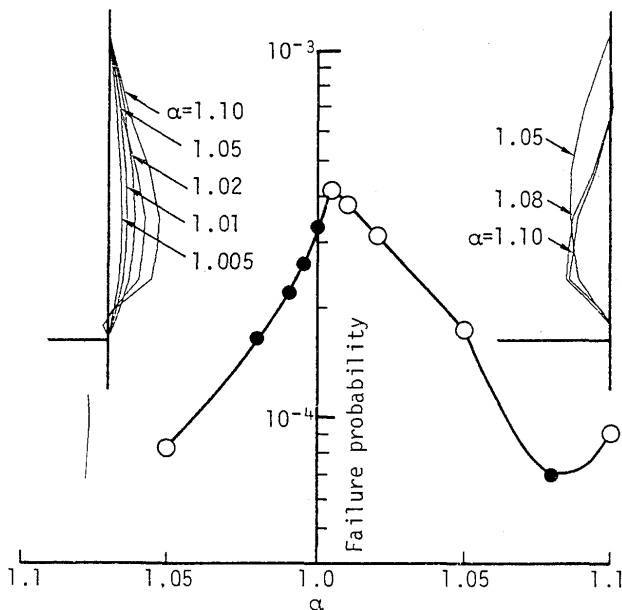Fig. 8   Distribution of the largest principal stress in the original model under thermal load.

Fig. 9   Optimum shapes and the failure probability under thermal load.
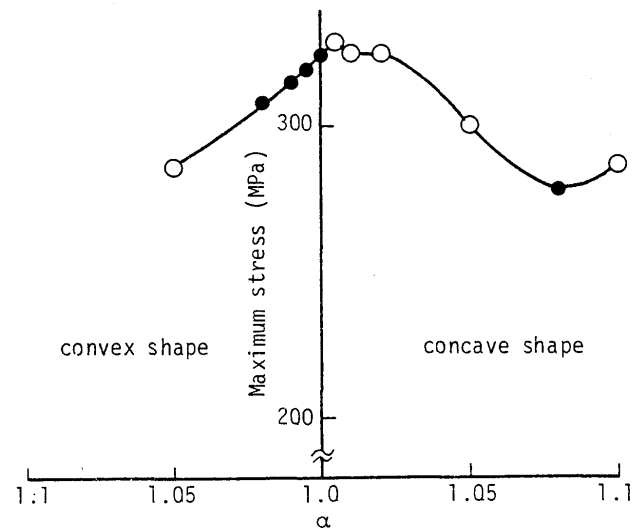

Fig. 10   Variation of the maximum stress in ceramics under thermal load with arc length factor.
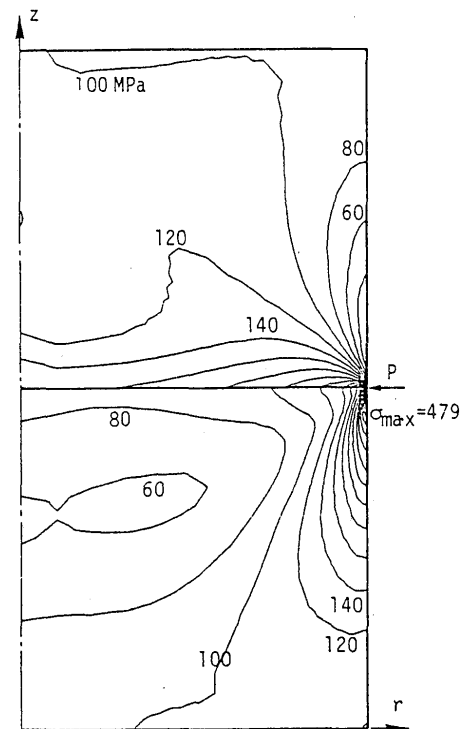
Fig. 11   Distribution of the largest principal stress in the original model under combined load.

tively.   The results of the optimization are shown for optimum shapes and failure probabilities in **Fig. 12**. Similarly, the relation between the arc length factor α and the maximum stress σ_{max} is shown in **Fig. 13**. It can be seen that only concave shape is effective to reduce the failure probability when both thermal and external loads are acting. The failure probability and the maximum stress when $\alpha=1.10$ are $P_f=3.23\times10^{-3}$ and

$\sigma_{max}=310$ MPa, respectively.   The distribution of the maximum principal stress for the same case is shown in **Fig. 14**. It is seen that the high stress region in the ceramic part shifts about 1 mm away from the interface.

3.5   Part of the optimization and its influence

Considering the machinability, the side of the metal part was chosen to be modified and the effectiveness of the shape optimization was discussed in the preceding sections. To clarify the effect of the location to be modified, the interface between ceramic and metal parts
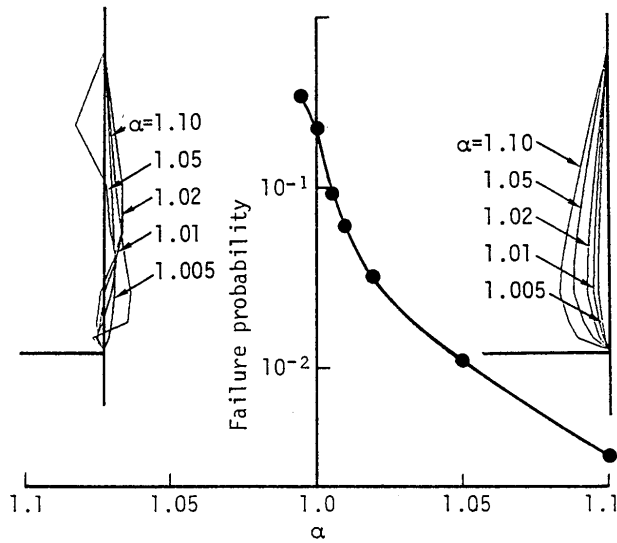
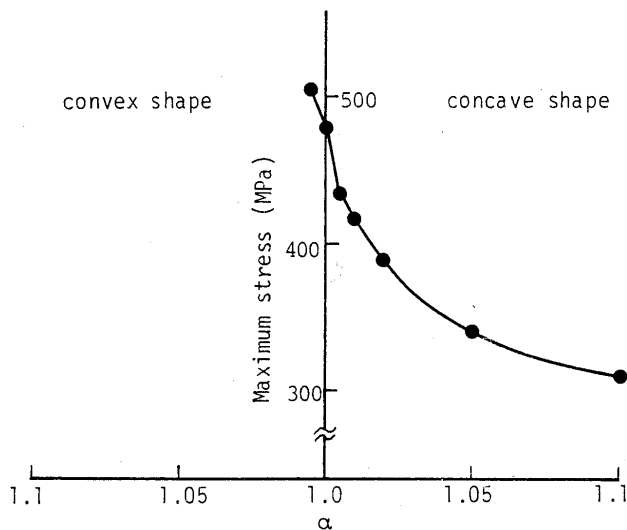Fig. 12 Optimum shapes and the failure probability under combined load.

Fig. 13 Variation of the maximum stress in ceramics under combined load with arc length factor.
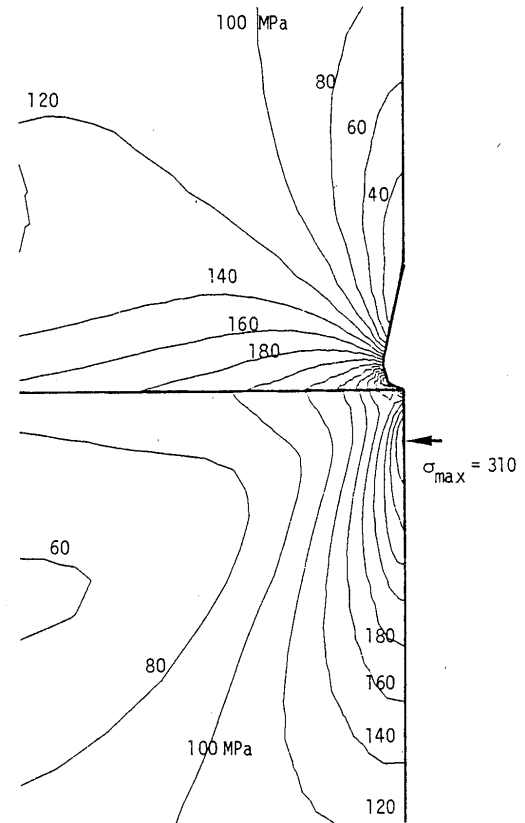

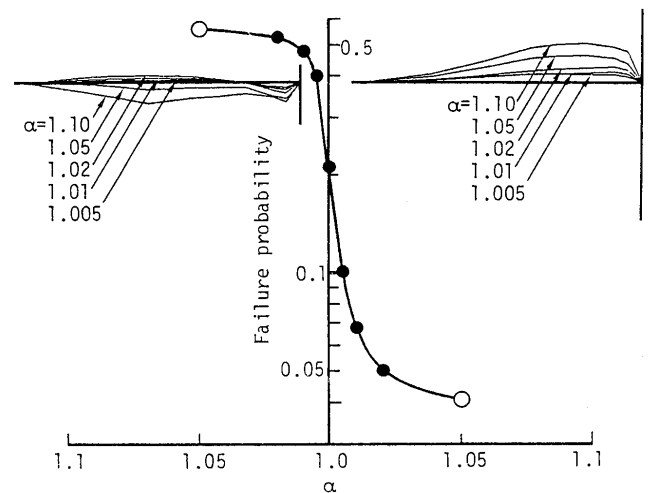Fig. 14 Distribution of the largest principal stress in the optimum shape under combined load ($\alpha = 1.10$).

Fig. 15 Optimum interface shapes and the failure probability under combined load.

is chosen as the part to be optimized. It is assumed that the thermal and the external loads are acting simultaneously in this case. The results of the optimization are shown in **Figs. 15** and **16**. The failure probability is reduced when the shape of the ceramic part at the interface is convex. On the contrary, if its shape is concave, the failure probability increases and also the obtained optimum shapes are not smooth.

Comparing these results with those for the cases in which the side surface of the metal part is modified, it can be seen that it is more effective to control the shape of the metal part than to control that of the interface. This conclusion agrees also with the numercal results obtained by the optimization in which the stress exceeding the allowable limit is minimized[4].

4. Conclusion

A shape optimization technique based on reliability is proposed as one of the means to reduce the failure probability of ceramics/metal joints. The mathematical formulations and the details of the computational procedures are presented in this report. Further, its effectiveness was demonstrated through simple numerical examples and it was shown that the shape optimiza-
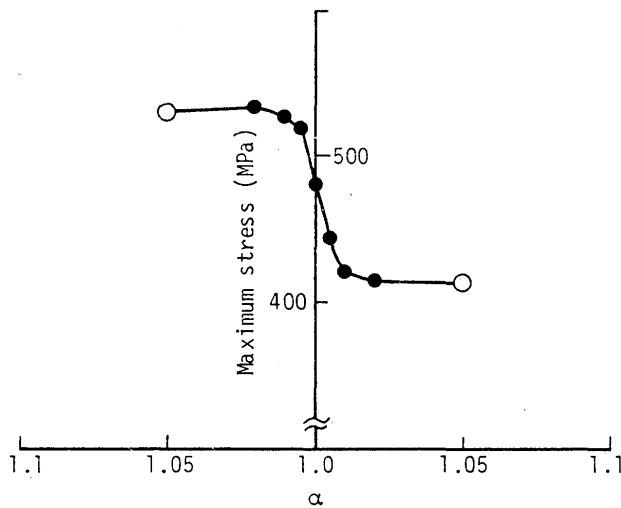
Fig. 16 Variation of the maximum stress in ceramics under combined load when the interface is modified.

tion can be an useful tool in designing ceramics/metal joints. Also, it is shown that the optimum shapes obtained based on the reliability show the same tendency as those reported in the previous report[4] for which

magnitude of the stress is directly used as the objective function.

References

1) K. Seo, M. Kusaka, F. Nogata, T. Terasaki, Y. Nakao and K. Saida, "Study on the Thermal Stress at Ceramics-Metal Joint", Trans. of Japan Society of Mechanical Engineers Series A, 55-510 (1989 in Japanese), 312-317.
2) H. Kobayashi, Y. Arai, H. Nakamura and M. Nakamura, "Mechanics Approach to Fracture Strength of Ceramics/Metal Joints", Trans. of Japan Society of Mechanical Engineers Series A, Vol. 55, No. 512 (1989 in Japanese), 750-755.
3) H. Koguchi, T. Kaya, Y. Ohtani and T. Yada, "Reliability Evaluation of Joints of Ceramics and Metals (3rd Report, Discussion and comparison for the effect of modification of joints geometry upon the thermal stress concentration by thermoelastic and thermoelastic-plastic analysis)", Trasn. of Japan Society of Mechanical Engineers Series A, Vol. 55, No. 513 (1989 in Japanese), 1121-1125.
4) H. Murakawa and Y. Ueda, "Shape Optimization for Reducing Stress at Ceramics/Metal Joints", Trans. JWRI, Vol. 18, No. 2 (1989), 133-140.
5) H. Murata, Y. Matsuo, M. Miyakawa and K. Kitakami, "Role of Fracture Diagnostic data in Estimation of parameters for Multimodal Weibull Distribution Function", Trans. of Japan Society of Mechanical Engineers Series A, Vol. 52, No. 473 (1986 in Japanese), 27-34.